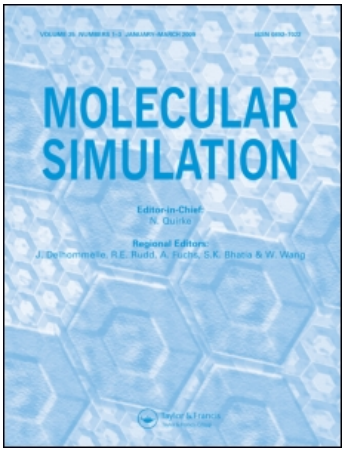

Molecular Simulation
Publication details, including instructions for authors and subscription information:
http://www.informaworld.com/smpp/title~content=t713644482

Effect of Confinement on Melting in Slit-Shaped Pores: Experimental and Simulation Study of Aniline in Activated Carbon Fibers

M. Śliwinska-Bartkowiak[a]; R. Radhakrishnan[b]; K. E. Gubbins[c]
[a] Institute of Physics, Adam Mickiewicz University, Poznan, Poland [b] Chemical Engineering Department, Massachusetts Institute of Technology, Cambridge, MA, USA [c] Department of Chemical Engineering, North Carolina State University, Raleigh, NC, USA

To cite this Article Śliwinska-Bartkowiak, M. , Radhakrishnan, R. and Gubbins, K. E.(2001) 'Effect of Confinement on Melting in Slit-Shaped Pores: Experimental and Simulation Study of Aniline in Activated Carbon Fibers', Molecular Simulation, 27: 5, 323 — 337
To link to this Article: DOI: 10.1080/08927020108031356
URL: http://dx.doi.org/10.1080/08927020108031356

Molecular Simulation, Vol. 27, pp. 323–337
Reprints available directly from the publisher
Photocopying permitted by license only

EFFECT OF CONFINEMENT ON MELTING IN SLIT-SHAPED PORES: EXPERIMENTAL AND SIMULATION STUDY OF ANILINE IN ACTIVATED CARBON FIBERS

M. ŚLIWINSKA-BARTKOWIAK[a], R. RADHAKRISHNAN[b] and K.E. GUBBINS[c,*]

[a]*Institute of Physics, Adam Mickiewicz University, ul Grunwaldzka 6, Poznan 60-780, Poland;* [b]*Chemical Engineering Department, Massachusetts Institute of Technology, Cambridge, MA 02139, USA;* [c]*Department of Chemical Engineering, North Carolina State University, Raleigh, NC 27695-7905, USA*

(Received June 2001; In final form July 2001)

We report both experimental and molecular simulation studies of the melting behavior of aniline confined within an activated carbon fiber having slit-shaped pores. Dielectric relaxation spectroscopy is used to determine the transition temperatures and also the dielectric relaxation times over the temperature range 240 to 340 K. For the confined system two transitions were observed, one at 298 K and a second transition at 324 K. The measured relaxation times indicate that the low temperature phase (below 298 K) is a crystalline or partially crystalline solid phase, while that above 324 K is a liquid-like phase; for the intermediate phase, in the range 298–324 K, the relaxation times are of the order 10^{-5} s, which is typical of a hexatic phase. The melting temperature of the confined system is well above that of bulk aniline, which is 267 K. The simulations are carried out using the Grand Canonical Monte Carlo method together with Landau free energy calculations, and phase transitions are located as state points where the grand free energies of two confined phases are equal. The nature of these phases is determined by analysis of in-plane pair positional and orientational correlation functions. The simulations also show two transitions. The first is a transition from a two-dimensional hexagonal crystal phase to a hexatic phase at 296 K; the second transition is from the hexatic to a liquid-like phase at 336 K. Confinement within the slit-shaped pores appears to stabilize the hexatic phase, which is the stable phase over a wider temperature range than for quasi-two-dimensional thin films.

Keywords: Melting; Aniline; Carbon fibers; Dielectric relaxation spectroscopy

*Corresponding author.

INTRODUCTION

Recent molecular simulation studies for pores of simple geometry have shown a rich phase behavior associated with melting and freezing in confined systems [1–9]. A review of the simulation and experimental work in this area up to 1999 has been given by Gelb *et al.* [8]. The freezing temperature may be lowered or raised relative to the bulk freezing temperature, depending on the nature of the adsorbate and the porous material. In addition, new surface-driven phases may intervene between the liquid and solid phases in the pore. "Contact layer" phases of various kinds often occur, in which the layer of adsorbed molecules adjacent to the pore wall has a different structure from that of the adsorbate molecules in the interior of the pore. For materials having walls that are weakly attractive (e.g. glasses, silicas) this contact layer is usually fluid-like while the interior molecules have adopted a crystalline structure. For materials such as carbon, which has walls that are strongly attractive, the contact layer is usually crystalline while the interior layers remain fluid. These contact layer phases have been predicted theoretically, and confirmed experimentally for several systems [3,7]. In addition, for some systems in which strong layering of the adsorbate occurs (e.g. slit pore models of activated carbon fibers), hexatic phases can occur; such phases have quasi-long-ranged orientational order, but positional disorder, and for quasi-two-dimensional systems occur over a temperature range between those for the crystal and liquid phases. These are clearly seen in molecular simulations [2,8], and preliminary experiments seem to confirm these phases [7,9]. Recently it has been shown [7,10] that this apparently complex phase behavior results from a competition between the fluid–wall and fluid–fluid intermolecular interactions. For a given pore geometry and width, the phase diagrams for a wide range of adsorbates and porous solids can be classified in terms of a parameter α that is the ratio of the fluid–wall to fluid–fluid attractive interaction [7,8,10].

In addition to the strong fundamental scientific interest, an understanding of freezing in confined systems is of practical importance in lubrication, adhesion, nano-tribology and fabrication of nano-materials. The use of nano-porous materials as templates for forming nano-materials such as nano-wires and nano-tube arrays is receiving wide attention. Recent examples have included the use of track-etched pores in anodized alumina to form nano-wire/nano-tube arrays [11], carbon nano-tubes for growing nano-wires [12], and opals to obtain aligned nano-particles [13,14]; formation of the nano-material in the porous template is usually achieved by infiltration of molten material [14], vapor phase deposition [15], or electrochemical deposition [16].

In this paper we report an experimental study of the freezing behavior of aniline confined within activated carbon fibers having a pore width of

approximately 1.8 nm. Dielectric relaxation spectroscopy is used to locate phase transitions, and to determine the dielectric relaxation time for confined aniline as a function of the temperature. Such relaxation times are a sensitive measure of the type of phase that is present, and the results indicate that two transitions occur on heating. We also report a molecular simulation study for a simple model of this system, in which the pores are represented as slit-shaped. Free energy calculations based on Landau theory, together with calculations of pair correlation functions, enable us to locate phase transitions and to determine the nature of the phases involved. The simulations indicate two transitions on heating, the first from a confined crystal to a hexatic phase, and the second from hexatic to liquid phase.

EXPERIMENTAL METHOD

Freezing of a dipolar liquid is accompanied by a rapid decrease in its electric permittivity [17–19]. After the phase transition to the solid-state dipole rotation ceases, and the electric permittivity is almost equal to n^2, where n is the refractive index of the solid, since it arises from deformation polarisation only. Therefore, dielectric spectroscopy is suited to the investigation of melting and freezing of dipolar liquids, because significant changes occur in the system's capacity at the phase transition. Investigation of the dynamics of a confined liquid is also possible from the frequency dependence of dielectric properties of such systems. Analysis of the frequency dependence of dielectric data allows a determination of the phase transition temperature of the adsorbed substance and also of characteristic relaxation frequencies related to molecular motion in particular phases [17–19].

The dielectric relaxation method was applied to study the process of freezing and melting of a sample of aniline confined in activated carbon fibres (ACF) of type P20, obtained from the laboratory of K. Kaneko. The ACF has pores that are approximately slit-shaped, with a mean pore size $H = 1.8\,\text{nm}$ [6]. The complex electric permittivity, $\kappa = \kappa' + i\kappa''$, where $\kappa' = C/C_0$ is the real, and $\kappa'' = \tan(\delta)/\kappa'$ is the complex part of the permittivity, was measured in the frequency interval 300 Hz–1 MHz at different temperatures by a Solartron 1200 impedance gain analyser, using a parallel plate capacitor made of stainless steel. In order to reduce the high conductivity of the sample, which was placed between the capacitor plates as a suspension of aniline filled ACF particles in pure liquid aniline, the electrodes were covered with a thin layer of teflon. From the directly measured capacitance, C, and the tangent loss $\tan(\delta)$, the values of κ' and κ'' were calculated for the known sample geometry [3,20]. The

temperature was controlled to an accuracy of 0.1 K using a platinum resistor Pt(100) as a sensor and a K30 Modinegen external cryostat coupled with a N-180 ultra-cryostat.

The aniline sample was twice distilled under reduced pressure and dried over Al_2O_3. The conductivity of purified aniline was on the order of $10^{-9}\,\Omega^{-1}\,m^{-1}$. The ACF material to be used in the experiment was heated to about 600 K, and kept under vacuum ($\sim 10^{-3}$ Torr) for 6 days prior to the introduction of the fluid.

For an isolated dipole rotating under an oscillating field in a viscous medium, the Debye dispersion relation is derived in terms of classical mechanics as:

$$\kappa = \kappa'_{\infty} + \frac{\kappa'_{s} + \kappa'_{\infty}}{1 + (i\omega\tau)}, \tag{1}$$

where ω is the frequency of the applied potential and τ is the orientational relaxation time of a dipolar molecule. The subscript s refers to static permittivity (low frequency limit, when the dipoles have enough time to be in phase with the applied field). The subscript ∞ refers to the high frequency limit, and is a measure of the induced component of the permittivity. The dielectric relaxation time was calculated by fitting the dispersion spectrum of the complex permittivity near resonance to the Debye model of orientational relaxation.

MOLECULAR SIMULATION METHOD

We have carried out Grand Canonical Monte Carlo (GCMC) simulations for a simple model of the aniline/ACF system, consisting of a Lennard–Jones fluid adsorbed in regular slit shaped pores of pore width H. Here H is the distance separating the planes through the centers of the surface-layer atoms on opposing pore walls. The fluid–fluid interaction between the adsorbed fluid molecules is modeled using the Lennard–Jones [6,12] potential. The fluid–wall interaction is modeled using a "10-4-3" Steele potential [21],

$$\phi_{fw>}(z) = 2\pi\rho_w\varepsilon_{fw}\sigma_{fw}^2\Delta\left[\frac{2}{5}\left(\frac{\sigma_{fw}}{z}\right)^{10} - \left(\frac{\sigma_{fw}}{z}\right)^{4} - \left(\frac{\sigma_{fw}^4}{3\Delta(z+0.61\Delta)^3}\right)\right] \tag{2}$$

Here, the σs and ϵs are the size and energy parameters in the LJ potential, the subscripts f and w denote fluid and wall respectively, ρ_w is the density of wall atoms, Δ is the spacing between successive layers of wall atoms, and z is the distance between the adsorbate atom and the nearest point in the wall. The carbon–carbon potential parameters and structural data were taken from Steele [21]. The values are: $\rho_w = 114\,nm^{-3}$, $\sigma_{ww} = 0.34\,nm$, $\varepsilon_{ww}/k = 28\,K$, $\Delta =$

0.335 nm. For a given pore width H, the total potential energy from both walls is given by

$$\phi_{\text{pore}}(z) = \phi_{\text{fw}}(z) + \phi_{\text{fw}}(H - z) \tag{3}$$

The intermolecular potential parameters were obtained as follows [7]. The intermolecular potential parameters for aniline–aniline interactions were obtained by fitting molecular simulation data for the bulk phase melting point at 1 atm pressure to experimental data [22,23]; this gave $\varepsilon_{\text{ff}}/k = 395\,\text{K}$, $\sigma_{\text{ff}} = 0.514\,\text{nm}$. This effective Lennard–Jones potential accounts for the dipolar forces in a crude way through the enlarged value of the well depth parameter. Lennard–Jones interactions were also used for the fluid–wall interactions. The parameters were estimated using the Lorentz–Berthelot combining rules; the above values were used for the carbon–carbon parameters, but for the aniline–aniline parameters we used those determined for the Stockmayer potential as fitted to second virial coefficients [24] so that the well depth parameter reflects the dispersion interaction without dipolar effects. These latter parameters for aniline were $\varepsilon_{\text{ff}}/k = 358\,\text{K}$, and $\sigma_{\text{ff}} = 0.514\,\text{nm}$.

The relative strength of the fluid–wall to the fluid–fluid interaction is determined by the parameter $\alpha = (2/3)\rho_{\text{w}}\varepsilon_{\text{fw}}\sigma_{\text{fw}}^2\Delta/\varepsilon_{\text{ff}}$.. In the case of aniline in activated carbon fibers, $\alpha = 1.2$. Our objective is to calculate the freezing temperatures in the confined phase to compare with the experimental results.

The simulation runs were performed in the grand canonical ensemble, fixing the chemical potential μ, the volume V of the pore, and the temperature T. A pore width of $H = 3\sigma_{\text{ff}}$ was chosen to enable comparison with our experimental results. A rectilinear simulation cell of dimensions $L \times L$ (where L equals $60\sigma_{\text{ff}}$) in the plane parallel to the pore walls was used. Typically, the system contained approximately 12,000 adsorbate molecules. The adsorbed molecules formed distinct layers parallel to the plane of the pore walls. The simulation was set up such that insertion, deletion and displacement moves were attempted with equal probability, and the displacement step was adjusted to have a 50% probability of acceptance. Thermodynamic properties were averaged over 2000 million individual Monte Carlo steps. The length of the simulation was adjusted such that a minimum of 50 times the average number of particles in the system would be inserted and deleted during a single simulation run.

The method for obtaining the free energy relies on the calculation of the Landau free energy as a function of an effective bond orientational order parameter Φ, using GCMC simulations [2]. The Landau free energy, Λ, is defined by,

$$\Lambda[\Phi] = -k_{\text{B}}T\ln(P[\Phi]) + \text{constant} \tag{4}$$

where $P[\Phi]$ is the probability of observing the system having an order parameter value between Φ and $\Phi + \delta\Phi$. The probability distribution function $P[\Phi]$ is calculated in a GCMC simulation as a histogram, with the help of umbrella sampling. The grand free energy Ω is then related to the Landau free energy by

$$\exp(-\beta\Omega) = \int d\Phi \exp(-\beta A[\Phi]) \tag{5}$$

The grand free energy at a particular temperature can be calculated by numerically integrating Eq. (5) over the order parameter space. We use a two-dimensional order parameter to characterize the order in each of the molecular layers.

$$\Phi_{6,j} = \left| \frac{1}{N_b} \sum_{k=1}^{N_b} \exp(i6\theta_k) \right| = |\langle \exp(i6\theta_k) \rangle j| \tag{6}$$

$\Phi_{6,j}$ measures the hexagonal bond order within each layer j. Each nearest neighbor bond has a particular orientation in the plane of the given layer, and is described by the polar coordinate θ. The index k runs over the total number of nearest neighbor bonds N_b in layer j. The overall order parameter Φ_6 is an average of the hexagonal order in all the layers. We expect $\theta_{6,j} = 0$ when layer j has the structure of a two-dimensional liquid, $\theta_{6,j} = 1$ in the two dimensional hexagonal crystal phase, and $0 < \Phi_{6,j} < 1$ in an orientationally ordered layer.

RESULTS

Experiment

The capacitance C and loss tangent $\tan(\delta)$ were measured as a function of frequency and temperature for bulk aniline and for aniline adsorbed in ACF, from which the dielectric permittivity $\kappa'(T,\omega)$ and the loss tangent $\kappa''(T,\omega)$ were calculated. Results of the measurements of C for bulk aniline as a function of T and at the frequency of 0.6 MHz are shown in Fig. 1. There is a sharp increase in C at $T = 267$ K, the melting point of the pure substance, due to the contribution to the orientational polarisation in the liquid state from the permanent dipoles [17,18]. In the frequency interval studied we could only detect the low-frequency relaxation of aniline. Analysis of the Cole–Cole representation of the complex permittivity for solid aniline has shown that the relaxation observed should be approximated by a symmetric distribution of relaxation times described formally by the Cole–Cole Eq. (1). Examples of the experimental results and the fitted

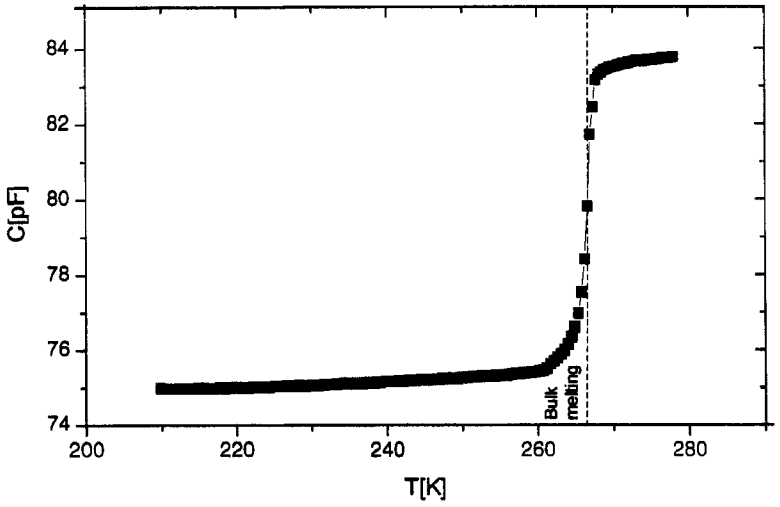

FIGURE 1 Capacitance, C, vs. temperature, T, for bulk aniline at $\omega = 0.6$ MHz.

curves are given in Fig. 2(a) for the bulk solid phase at 260 K. From the plot of κ' and κ'' vs. $\log_{10}(\omega)$ the relaxation time can be calculated as the inverse of the frequency corresponding to a saddle point of the κ' plot or a maximum of the κ'' plot. An alternative graphical representation of the Debye dispersion equation is the Cole–Cole diagram in the complex κ plane, shown in Fig. 2(b). Each relaxation mechanism is reflected as a semicircle in the Cole–Cole diagram. From the plot of κ'' vs. κ', the value of τ is given as the inverse of the frequency at which κ'' goes through a maximum.

In Fig. 3 the variation of the relaxation time with temperature is presented for bulk aniline, as obtained from fitting Eq. (1) to the dispersion spectrum. In the solid phase (below 267 K), our measurements showed a single relaxation time of the order of 10^{-3}–10^{-4} s in the temperature range from 240 to 267 K. The liquid branch above 267 K has rotational relaxation times of the order of 10^{-11} s [17,18]. This branch lies beyond the possibilities of our analyser. In the presence of dipolar constituents, one or more absorption regions are present, not all of them necessarily associated with the dipolar dispersion. At the lowest frequencies (especially about 1 KHz), a significantly large κ'' value arises from the conductivity of the medium and interfacial (Maxwell–Wagner) polarisation is found if the system is not in a single homogeneous phase. For aniline, a homogeneous medium whose conductivity is of the order of $10^{-9}\,\Omega^{-1}\,m^{-1}$, the absorption region observed for the frequencies 1–10 KHz is related to the conductivity of the medium. The Joule heat arising from the conductivity contributes to a loss factor κ'' (conductance) so the value at low frequency is:

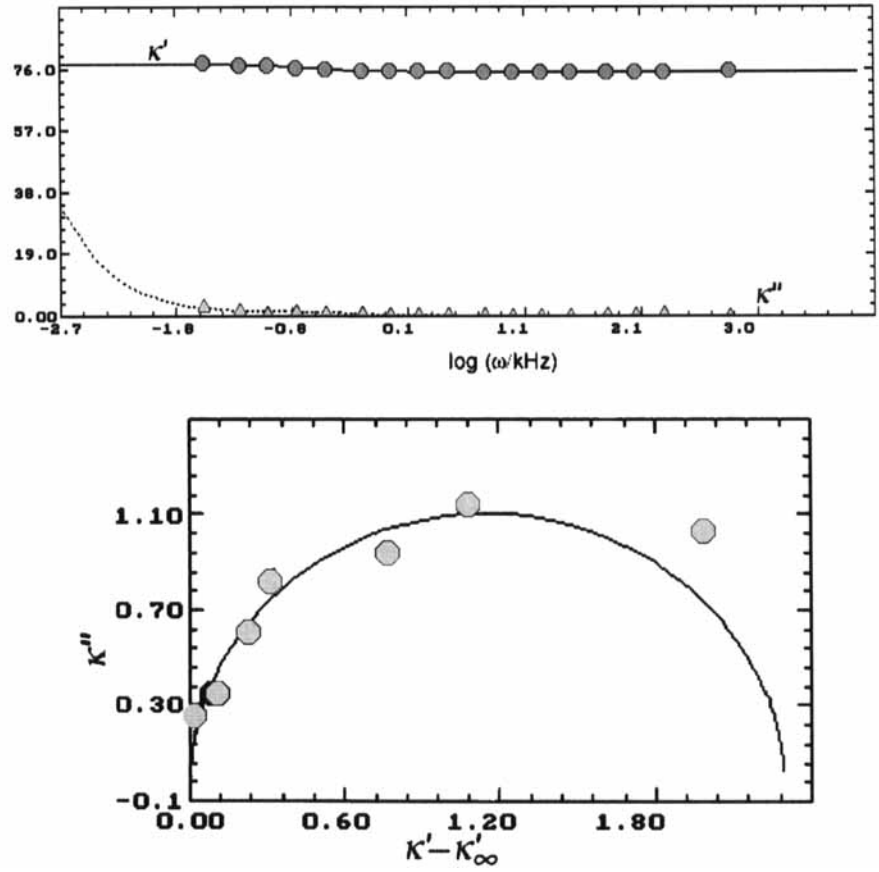

FIGURE 2 (a) Spectrum plot for aniline at 260 K. The solid and the dashed curves are fits to the real and imaginary parts of κ. (b) Representation of the spectrum plot in the form of a Cole–Cole diagram for bulk aniline at 260 K.

κ''(total) = κ''(dielectric) + κ''(conductance), and the system reveals the energy loss in processes other than dielectric relaxation. In Fig. 3 the branch above 267 K, corresponding to relaxation times of the order of 10^{-2} s, characterises the process of adsorption related to the conductivity of the medium. This branch is characteristic of the liquid phase and is a good indicator of the appearance of this phase.

The behavior of C vs. T for aniline in ACF at a frequency of 0.6 MHz is shown in Fig. 4. The sample was introduced between the capacitor plates as a suspension of ACF in pure aniline. The sharp increase in C at 267 K seen in Fig. 4(a) is due to the bulk solid–liquid transition, and we do not observe additional changes of C characteristic of phase transitions for temperatures lower than the bulk melting

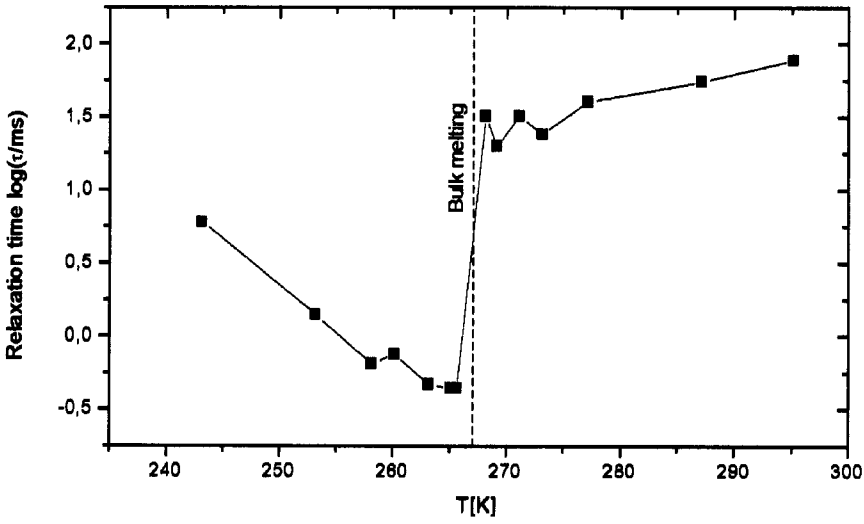

FIGURE 3 Dielectric relaxation time, τ, vs. temperature for bulk aniline.

point. The behavior of C vs. T for aniline in ACF at temperatures in the range 290–340 K for frequencies of 0.01, 0.1 and 1 MHz is shown in Fig. 4(b). In this temperature range we observe two sudden changes in C that are not observed in the case of bulk aniline, and must be related to changes in the aniline confined within ACF. These changes occur at 298 and 324 K, and indicate phase or structural transitions in the confined phase. The latter change is very similar to that corresponding to the melting of a dipolar liquid placed in porous glass [3,20], where a significant increase in C indicated a phase transition to the liquid phase. These results suggest that the melting process of aniline confined in ACF has two steps: from solid to intermediate phase (at 298 K), and from intermediate phase to liquid at 324 K.

The characteristic relaxation times related to molecular motion in particular phases are presented at Fig. 5, where the behavior of the relaxation times as a function of temperature for aniline in ACF is depicted. For the temperature range 273–340 K there are several different kinds of relaxation. The larger component of the relaxation time of the order 10^{-2} s is related to the conductivity of aniline in pores and testifies to the presence of a liquid phase in the system. This component appears at 324 K, where the second transition was observed in Fig. 4(b). A relaxation time related to the Maxwell–Wagner polarisation, of the order 10^{-3} s and characteristic of interfacial polarisation, is observed over the whole temperature range. At temperatures below 298 K we observe a relaxation time of the order 10^{-4} s, which is typical of the aniline solid (crystal) phase.

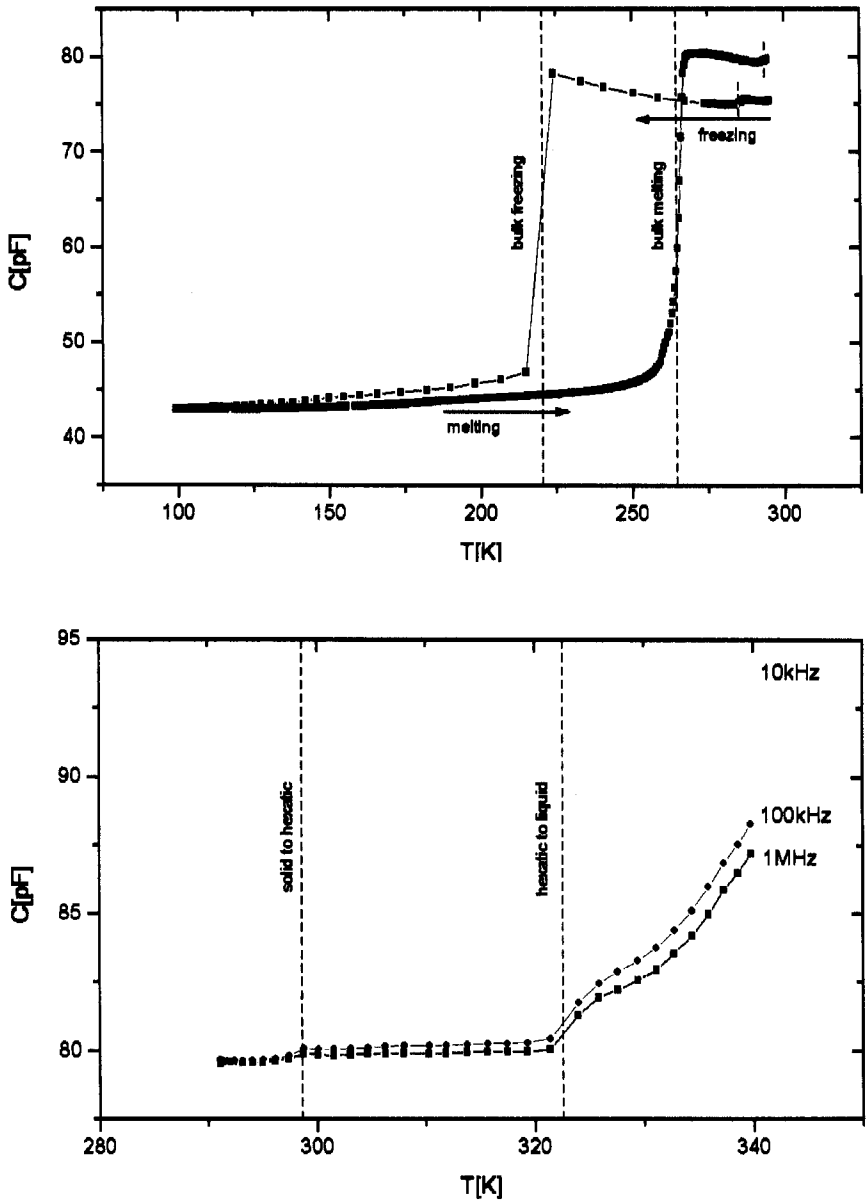

FIGURE 4 (a) Capacitance vs. temperature for aniline in ACF at frequency $\omega = 0.6$ MHz at lower temperatures, (b) C vs. T for aniline in ACF at different frequencies for temperatures 290–340 K.

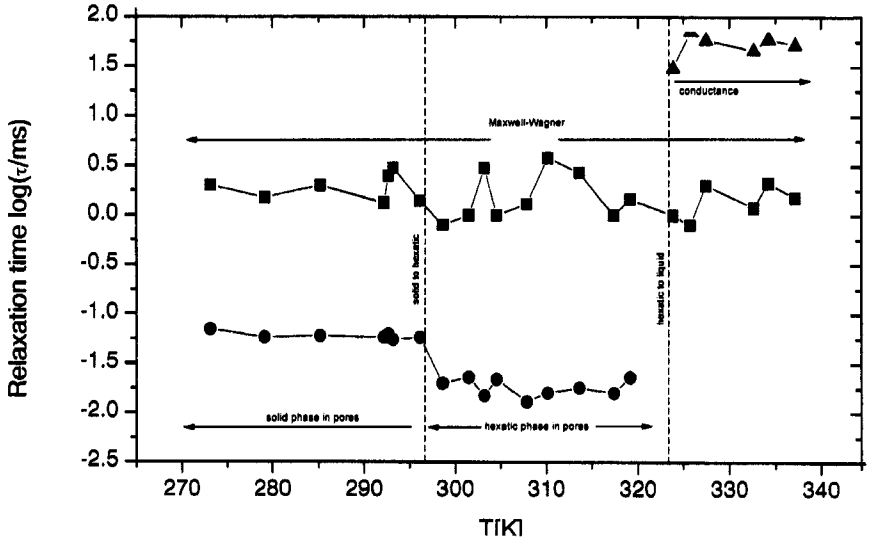

FIGURE 5 Dielectric relaxation times, τ vs. T for aniline in ACF.

Above this temperature, in the range 298–324 K, a branch of relaxation time of the order 10^{-5} s appears. This branch can be related to a Debye-type dispersion in the intermediate phase, which could be a hexatic phase [20].

Simulation Results

The reduced melting temperature of the bulk Lennard–Jones fluid at 1 atm. pressure is $k_B T_f/\varepsilon_{ff} = 0.682$. For our model of aniline this corresponds to a melting temperature of 269 K, very close to the experimental value of 267 K. During the course of our GCMC simulations the distribution function $P[\Phi]$ was calculated as a function of Φ, and hence the Landau free energy and grand free energy were obtained from Eqs. (4) and (5), respectively. At most temperatures, the Landau free energy plots versus Φ showed three local minima, corresponding to three phases. At a given temperature, one of these minima was the global one, indicating the thermodynamically stable phase at that temperature; at temperatures at which two of the phases were in thermodynamic equilibrium two of these minima had the same Landau free energy. The state conditions of phase coexistence were determined by requiring the grand free energies of the two confined phases to be equal.

The resulting grand free energy curves for the three phases are shown in Fig. 6. Two thermodynamic phase transitions are observed, one at 296 K and the other at

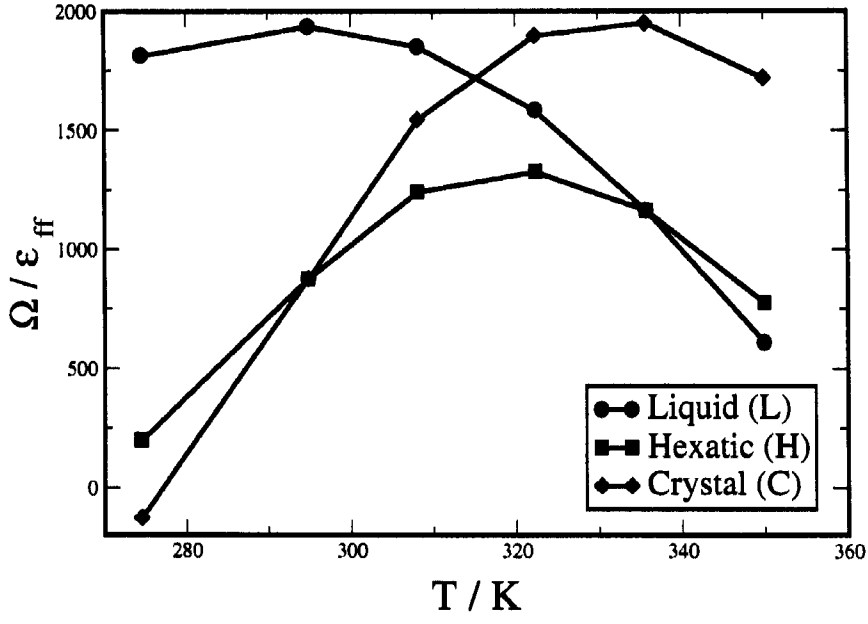

FIGURE 6 Grand free energy vs temperature for the three phases observed, from molecular simulation.

336 K. The phase transitions are seen to be first order, at least for this size of simulation box. These free energies give no information about the nature of the phases involved. However, we note that in these confined systems, because of the slit-shaped pore and narrow pore width, the adsorbate molecules are confined to layers that are quasi-two-dimensional systems. Nelson and Halperin [25] proposed the KTHNY (Kosterlitz–Thouless–Halperin–Nelson–Young) mechanism for the melting of a two-dimensional crystal in two dimensions, which involves two transitions of the Kosterlitz–Thouless [26] type. The first is a transition from the two-dimensional crystal phase, with quasi-long range positional order and long-range orientational order, to a hexatic phase with long-range orientational order but positional disorder; the second transition is from the hexatic phase to a liquid (having neither long range positional or orientational order). The hexatic phase was first observed experimentally in electron diffraction experiments on liquid crystalline thin films [27]. Molecular simulation studies by Zangi and Rice [28] for quasi-two dimensional films in which some out of plane motion is permitted showed two phase transitions as proposed by the KTHNY mechanism, with the hexatic phase as the intermediate one between crystal and liquid.

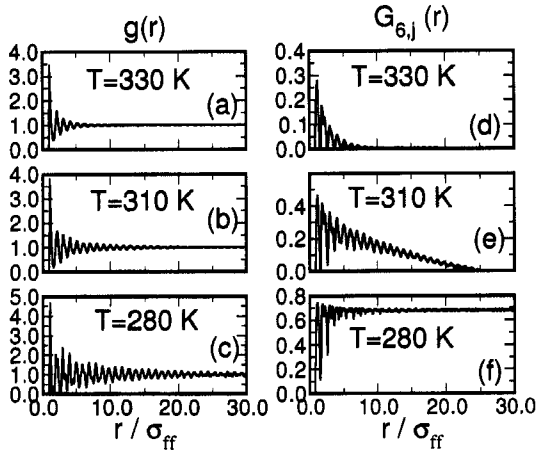

FIGURE 7 Pair correlation functions in the two confined molecular layers of aniline in ACF from simulation: (a) $g(r)$ in the liquid phase; (b) $g(r)$ in the hexatic phase; (c) $g(r)$ in the crystal phase; (d) $G_{6j}(r)$ in the liquid phase; (e) $G_{6j}(r)$ in the hexatic phase; (f) $G_{6j}(r)$ in the crystal phase.

In order to determine the nature of the phases shown in Fig. 6 we calculated the in-plane pair positional and orientational correlation functions at each temperature, since these provide a clear signature of fluid, crystal and hexatic phases. Typical results are shown in Fig. 7 for temperatures in the stable regions of the three different phases. In this figure $g(r)$ is the usual two-dimensional in plane pair correlation function, or radial distribution function. The orientational pair correlation function, $G_{6j}(r)$, for the confined molecular layer j is defined as

$$G_{6,j}(r) = \langle \Phi^*_{6j}(0)\Phi_{6,j}(r)\rangle \tag{7}$$

At the highest temperature, 330 K, the $g(r)$ is isotropic in nature with a rapid damping of the oscillations, while the orientational correlation function shows exponential decay; these are signatures of a fluid or liquid phase. At the intermediate temperature of 310 K the $g(r)$ is isotropic, with oscillations that are longer in range, while the orientational correlation function decays algebraically, i.e. as $1/r$; this is a clear signature of a hexatic phase with short range positional order, but quasi-long range orientational order. At the lowest temperature of 280 K the $g(r)$ is anisotropic and typical of a somewhat disordered crystal, while the orientational correlation function shows long range order, again indicating a crystal phase. Examination of snapshots showed that the low temperature phase had a 2-D hexagonal crystal structure.

DISCUSSION AND CONCLUSIONS

Both the experimental and simulation results show that aniline confined within ACF melts at a temperature higher than the bulk value of 267 K. The experiment gave a melting temperature for the confined system of 298 K, while simulation gave 296 K, an elevation due to confinement of 31 and 29 K, respectively. Such an increase is expected based on our knowledge of the global freezing behavior [7] in view of the high value of $\alpha = 1.2$ for this system, and is consistent with other experimental results for confinement in ACF [5–9].

The experiments show two transitions for the confined system, one at 298 and the second at 324 K. Analysis of the dielectric relaxation times for the three phases shows that for temperatures below 298 they are characteristic of a crystal aniline phase, while above 324 K they are characteristic of liquid phases. For the intermediate phase, between 298 and 324 K, the dielectric relaxation times are of the order 10^{-5} s, which is of the order found for hexatic phases. The simulations also show two transitions, at 296 and 336 K, respectively. Analysis of the positional and orientational pair correlation functions shows that the intermediate phase is a hexatic phase, and is the stable phase between 296 and 336 K; thus the lower transition temperature corresponds to melting of the hexagonal crystal to a hexatic phase, while the upper transition temperature is for a hexatic to liquid transition.

The molecular models used in the simulations (slit pore, smooth walls, simple Lennard–Jones potentials) are crude. Nevertheless we believe they capture the physics involved in these transitions. There is good qualitative agreement between the experiment and simulation, and even fairly good quantitative agreement. The results suggest that confinement within narrow slit pores having strongly adsorbing walls, thus enforcing strong layering of the adsorbate, promotes the stability of a hexatic phase, so that it can be observed for simple adsorbate molecules over a rather wide temperature range, 26 K in the experimental system. This is in contrast to previous studies, which have usually been for thin films of liquid crystal phases, where the hexatic phase is only stable over a narrow temperature range. Thus, such confined systems seem promising for further study of hexatic phases.

Acknowledgements

This work was supported by grants from the National Science Foundation (grant no. CTS-9908535) and KBN. Supercomputer time was provided under a NSF/NRAC grant (MCA93S011).

References

[1] Miyahara, M. and Gubbins, K.E. (1997) "Freezing/melting phenomena for Lennard–Jones methane in slit pores: a Monte Carlo study", *J. Chem. Phys.* **106**, 2865–2880.

[2] Radhakrishnan, R. and Gubbins, K.E. (1999) "Free energy studies of freezing in slit pores: an order-parameter approach using Monte Carlo simulation", *Mol. Phys.* **96**, 1249–1267.

[3] Śliwinska-Bartkowiak, M., Gras, J., Sikorski, R., Radhakrishnan, R., Gelb, L.D. and Gubbins, K.E. (1999) "Phase transitions in pores: experimental and simulation studies of melting and freezing", *Langmuir* **15**, 6060–6069.

[4] Dominguez, H., Allen, M.P. and Evans, R. (1998) "Monte Carlo studies of the freezing and condensation transitions of confined fluids", *Mol. Phys.* **96**, 209–229.

[5] Kaneko, K., Watanabe, A., Iiyama, T., Radhakrishnan, R. and Gubbins, K.E. (1999) "A remarkable elevation of freezing temperature of CCl_4 in graphitic micropores", *J. Phys. Chem. B* **103**, 7061–7063.

[6] Radhakrishnan, R., Gubbins, K.E., Watanabe, A. and Kaneko, K. (1999) "Freezing of simple fluids in microporous activated carbon fibers: comparison of simulation and experiment", *J. Chem. Phys.* **III**, 9058–9067.

[7] Radhakrishnan, R., Gubbins, K.E. and Śliwinska-Bartkowiak, M. (2000) "Effect of the fluid–wall interaction on freezing of confined fluids: towards the development of a global phase diagram", *J. Chem. Phys.* **112**, 11048–11057.

[8] Gelb, L.D., Gubbins, K.E., Radhakrishnan, R. and Śliwinska-Bartkowiak, M. (1999) "Phase separation in confined systems", *Rep. Prog. Phys.* **62**, 1573–1659.

[9] Śliwinska-Bartkowiak, M., Dudziak, G., Sikorski, R., Gras, R., Gubbins, K.E. and Radhakrishnan, R. (2001) "Dielectric studies of freezing behavior in porous materials: water and methanol in activated carbon fibers", *Phys. Chem. Chem. Phys.* **3**, 1179–1184.

[10] Radhakrishnan, R., Śliwinska-Bartkowiak, M., Gubbins, K.E. (2001) "Global phase diagrams for freezing in porous media", *J. Chem. Phys.* submitted (2000).

[11] Masuda, H. and Fukuda, K. (1995) "Ordered metal nanohole arrays made by a two-step replication of honeycomb structures of anodic alumina", *Science* **268**, 1466–1468.

[12] Harris, P.J.F. (1999) Carbon Nanotubes and Related Structures. New Materials for the Twenty-first Century (Cambridge University Press, New York).

[13] Zhakidov, A.A., Baughman, R.H., Iqbal, Z., Cui, C.X., et al., (1998) "Carbon structures with three-dimensional periodicity at optical wavelength", *Science* **282**, 897–901.

[14] Zhang, Z.B., Gekhtman, D., Dresselhaus, M.S. and Ying, J.Y. (1999) "Processing and characterization of single-crystalline ultrafine bismuth nanowires", *Chem. Mater.* **II**, 1659–1665.

[15] Heremans, J., Thrush, C.M., Lin, Y.M., Cronin, S., et al., (2000) "Bismuth nanowire arrays: synthesis and galvanometric properties", *Phys. Rev. B* **61**, 2921–2930.

[16] Liu, K., Chien, C.L., Searson, P.C. and Kui, Y.Z. (1998) "Structural and magneto-transport properties of electrodeposited bismuth nanowires", *Appl. Phys. Lett.* **73**, 1436–1438.

[17] Hill, N., Vaughan, W.E., Price, A.H. and Davies, M. (1970) "Dielectric properties and molecular behaviour", Sugden, T.M., ed, (Van Nostrand Reinhold Co., New York).

[18] Ahadov, A.U. (1975) Dielektricieskoje svoistva tchistih zhidkosti (Izdaitelstwo Standardow, Moskva).

[19] Szurkowski, B., Hilczer, T. and Śliwinska-Bartkowiak, M. (1993), *Berichte Bunsenges. Phys. Chem.* **97**, 731.

[20] Śliwinska-Bartkowiak, M., Dudziak, G., Sikorski, R., Gras, R., Radhakrishnan, R. and Gubbins, K.E. (2001) "Melting/freezing behavior of a fluid confined in porous glasses and MCM-41: dielectric spectroscopy and molecular simulation", *J. Chem. Phys.* **114**, 950–962.

[21] Steele, W.A. (1973), *Surf. Sci.* **36**, 317.

[22] Kofke, D. (1993), *J. Chem. Phys.* **98**, 4149.

[23] Agrawal, R. and Kofice, D. (1995), *Mol. Phys.* **85**, 43.

[24] Hirschfelder, J.O., Curtiss, C.F. and Bird, R.B. (1954) Molecular Theory of Gases and Liquids (Wiley, New York).

[25] Nelson, D.R. and Halperin, B.I. (1979), *Phys. Rev. B* **19**, 2457.

[26] Kosterlitz, J.M. and Thouless, D.J. (1973), *J. Phys. C* **6**, 1181.

[27] Brock, J.D., Birgenau, R.J., Lister, J.D. and Aharony, A. (1989), *Phys. Today* **July**, 52.

[28] Zangi, R. and Rice, S.A. (1998), *Phys. Rev. E* **58**, 7529.